Int. J. Electrochem. Sci., 13 **(2018)** 4526 – 4534, doi: 10.20964/2018.05.45

International Journal of
ELECTROCHEMICAL
SCIENCE
www.electrochemsci.org

Two-step Synthesis of $LiVP_2O_7$/C for Use as Cathode Material in Lithium-Ion Batteries

Huayi Yu[1], *Zhi Su*[1,2,*], *Hualing Tian*[1,2]

[1]College of Chemistry and Chemical Engineering, Xinjiang Normal University, Urumqi, 830054, Xinjiang, China
[2]Engineering Research Center Of Electrochemical Technology and Application, Xinjiang Normal University, Urumqi, 830054, Xinjiang, China
[*]E-mail: suzhixj@sina.com

Received: 11 January 2018 / *Accepted:* 7 March 2018 / *Published:* 10 April 2018

$LiVP_2O_7$/C was synthesized by a novel two-step method, which involves combining the sol-gel method and the high-temperature solid phase method. VP_2O_7, $VOPO_4$, and $LiVOPO_4$ were used as the precursors for producing the $LiVP_2O_7$/C composite. The electrochemical performances of the three samples synthesized using the different precursors were compared. It was found that $LiVP_2O_7$/C prepared using VP_2O_7 as the precursor showed the best electrochemical performance. The initial discharge capacity of this sample was 100.2 $mAh \cdot g^{-1}$, while its discharge capacity was 90.8 $mAh \cdot g^{-1}$ after 50 cycles. Moreover, this $LiVP_2O_7$ sample exhibited a high voltage platform of approximately 4.2 V/4.3 V.

Keywords: $LiVP_2O_7$/C; cathode materials; two-step synthesis method

1. INTRODUCTION

The ongoing energy crisis and environmental pollution are arguably two of the greatest challenges faced by society today. To solve these problems, it is imperative to develop novel clean and renewal secondary energy sources. As a recyclable green energy source, lithium-ion batteries are attracting ever-increasing attention and have already found wide applicability [1, 2]. The performance and production cost of the cathode material, which is the primary component of lithium-ion batteries, directly determines their suitability for various applications. Therefore, it is critical to develop suitable cathode materials [3, 4]. At present, the commercial cathode materials of lithium-ion batteries include $LiCoO_2$ [5, 6], $LiMn_2O_4$ [7, 8], and $LiFePO_4$ [9, 10]. Based on the properties of $LiFePO_4$, other polyanionic cathode materials have also been developed. As a result, several other polyanionic

compounds have been synthesized in recent years. Among these is the new polycationic pyrophosphate cathode material $Li_{2-x}MP_2O_7$ [11-14]. $LiMP_2O_7$ (M = Fe, V) cathodes were first studied in the early 2000s. These materials have a more stable P_2O_7 group, which is formed by the cross-linking of two PO_4 groups. However, they suffer from poor electrochemical properties because of their high molecular weight, poor electronic conductivity, and low ion-diffusion rate [11]. Subsequently, after a break of several years, Nishimura et al. discovered a novel pyrophosphate material, $Li_2FeP_2O_7$. They evaluated its electrochemical properties and found that it has a reversible capacity of approximately 110 $mAh \cdot g^{-1}$ and that its potential plateaus at 3.5 V [15]. Since then, several other researchers have also investigated pyrophosphate materials [16-21].

In most previous studies on these materials, the materials were synthesized using the high-temperature solid method. However, the electrochemical properties of the materials prepared using this method are less than desirable and need significant improvements. Wurm et al. prepared $LiVP_2O_7$ by the ball-milling method and reported that the reversible capacity of the resulting material was 50 $mAh \cdot g^{-1}$ at 0.05C [22]. Zheng et al. also synthesized $LiVP_2O_7$ by the ball-milling method in 2016 and reported that the initial discharge capacity of the synthesized $LiVP_2O_7$ sample was 46.3 $mAh \cdot g^{-1}$ at 0.1C [23]. So these reports showed that the electrochemical properties of $LiVP_2O_7$ were poor.

And we present two new methods of $LiVP_2O_7$ preparation, which solve shortcomings of the previous methods. One is the two step method of this article, and another is the sol-gel method which is published in Ceramics International [24].

Because $LiVP_2O_7$ material has two short comings, one is its poor electronic conductivity, and the other is its low ion-diffusion rate. However, carbon coating has successfully solved poor conductivity of $LiVP_2O_7$ material [25].

In here, $LiVP_2O_7$/C was synthesized as a cathode material using a two-step method which combines the sol-gel method and the high-temperature solid phase method, making the proposed approach a novel one for synthesizing $LiVP_2O_7$/C. The first step was to prepare the precursor by the so-gel method, as this allows for control over grain growth and hence the synthesis of nanoparticles. In the second step, the uniform $LiVP_2O_7$/C powder was sintered. The electrochemical properties of $LiVP_2O_7$/C samples prepared using three different precursors were compared. It was found that the $LiVP_2O_7$/C sample prepared using the precursor VP_2O_7 showed the best electrochemical performance.

2. EXPERIMENTAL

2.1. Synthesis process

2.1.1. Preparation of VP_2O_7 and $LiVP_2O_7$/C

To begin with, V_2O_5 was dissolved in H_2O_2. Once the solution had turned orange, a mixed solution of citric acid and H_3PO_4 was added to it in a drop-by-drop manner. A dark green sol was obtained after magnetic stirring for 4 h.

Next, the sol was placed in a drying oven at 80 °C for 12 h, resulting in a brown gel, which was sintered at 700 °C for 2 h in muffle furnace to obtain VP_2O_7. Next, stoichiometric amounts of VP_2O_7, Li_2CO_3, and citric acid were dissolved in deionized water, and then used a planetary ball mill to mill them. The mass ratio of the powder, deionized water, and the beads was 1:1:5. Milling was performed at the speed of 400 rpm for 6 h. After the evaporation of the water, the mixed powder was presintered at 350 °C for 4 h and then sintered at 750 °C for 8 h in a tube furnace to obtain $LiVP_2O_7$/C. The obtained product is labeled S1.

2.1.2. Preparation of $VOPO_4$ and $LiVP_2O_7$/C

$VOPO_4$ was synthesized at 450 °C for 6 h in air using the above-described method. The mixture obtained after milling using a planetary ball mill was dried at 80 °C for 12 h. This powder was then presintered at 350 °C for 4 h and subsequently sintered at 750 °C for 8 h in a tube furnace to get the $LiVP_2O_7$/C. The obtained product is labeled S2.

2.1.3. Preparation of $LiVOPO_4$ and $LiVP_2O_7$/C

In this case, first, $LiVOPO_4$ was synthesized by heating at 600 °C for 10 h in Ar by the above-mentioned method using $LiNO_3$, V_2O_5, H_3PO_4, and citric acid as the starting materials. Next, the requisite amounts of $LiVOPO_4$ and citric acid were mixed and milled using a planetary ball mill. After being dried at 80 °C for 12 h, the mixed powder was presintered at 350 °C for 4 h and then sintered at 750 °C for 8 h in a tube furnace to obtain $LiVP_2O_7$/C. The obtained product is labeled S3.

2.2. Characterization

The phases of the $LiVP_2O_7$/C materials were analyzed using X-ray diffraction (XRD) analyses (Bruker D2), which were performed using Cu Ka radiation (30 kV, 10 mA) for 2θ values of 10–70° at a scan rate of 0.02°/s. Further, scanning electron microscopy (SEM, Hitachi SU8220), and transmission electron microscopy (TEM, Jeol JEM-2010FEF) were also performed on samples. In addition, elemental analyses (Vario EL III, Elementar) were performed to confirm the carbon contents of the final products. X-ray photoelectron spectroscopy (XPS, ESCALAB 250Xi) was used to assess the each element electronic state of resulting material.

Next, the samples were used to prepare coin-type cells (LIR2025), which were subjected to electrochemical measurements. The measurements were performed in a glove box. The cathode electrodes were prepared using a mixture consisting of active material, acetylene black and polytetrafluoroethylene. The obtained muld was cast onto an aluminum current collector, and disks 10 mm in diameter were cut and dried at 110 °C for 12 h. The electrolyte used consisted of a solution of 1 M $LiPF_6$ in ethylene methyl carbonate/ethylene carbonate/ dimethyl carbonate in a volume ratio of 1:1:1.

Charge/discharge and cycling tests were performed using a battery tester (LAND CT-2001A) for voltages of 2.5–4.5 V. The Cyclic voltammetry and AC impedance of the $LiVP_2O_7$/C materials were performed using an electrochemical workstation (Chenhua CHI 650D) at the scan rate of 0.1 $mV \cdot s^{-1}$, and the voltage range is 2.5-4.5 V. The frequencies ranged from 0.01 Hz to 0.1 MHz.

3. RESULTS AND DISCUSSION

The XRD patterns of VP_2O_7, $VOPO_4$, and $LiVOPO_4$ are shown in Fig. 1(a-c). As can be seen, there are not impurity peaks, and all the diffraction peaks can be indexed to the standard cards. Figure 1(d) shows the XRD patterns of three samples obtained using the three different precursors. It can be seen clearly that the diffraction peaks of all three samples are sharp and can be indexed to monoclinic $LiVP_2O_7$ (JCPDS: 85-2381). Further, no peaks related to carbon in the XRD patterns, indicating that the $LiVP_2O_7$ samples consisted of a single phase and that the carbon in the samples was amorphous and uniformly attached to the particles [26].

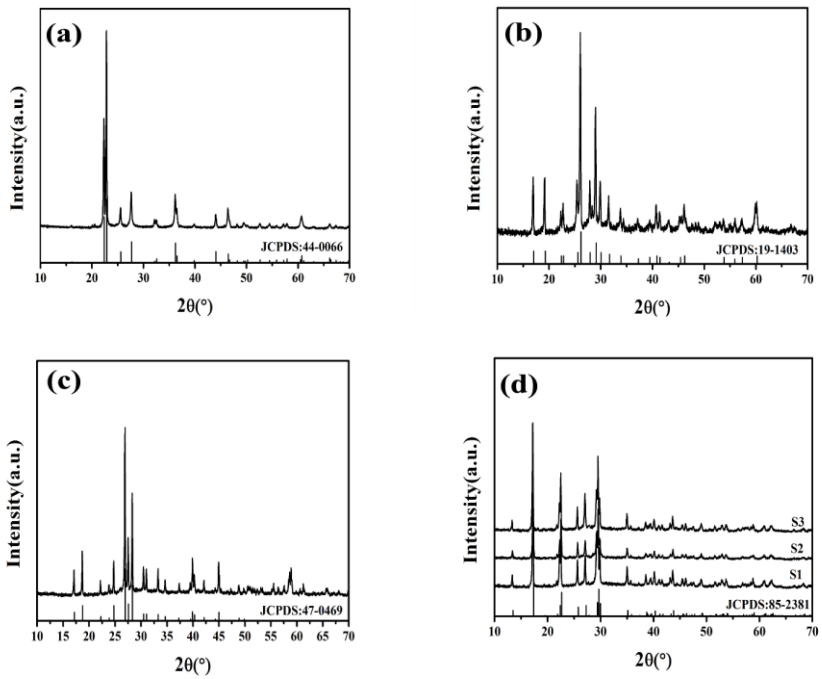

Figure 1. XRD patterns of (a) VP_2O_7, (b) $VOPO_4$, (c) $LiVOPO_4$, and (d) $LiVP_2O_7$/C samples (S1 to S3).

SEM images of the three samples are shown in Fig. 2(a), (c) and (e). The images indicate that the samples consist of irregular block-shaped particles. Furthermore, S1 exhibits the smallest particle size, owing to the calcination time of its precursor being the shortest. Further, the particles of S2 and S3 show slight agglomeration, with S3 having the largest particle size, as the calcination time in this case was the highest. The large particle size would probably prevent the diffusion of lithium ions and have a negative effect on the electrochemical performance. Figures 2(b), (d) and (f) show TEM images

of the S1, S2 and S3. As can be seen that a carbon layer covers the surfaces of the sample particles, with the coating thickness for S1, S2, and S3 being 2.52, 1.96, and 2.01 nm, respectively. Furthermore, the results of the elemental analyses indicated that the carbon contents of S1, S2, and S3 were 3.88%, 3.74%, and 3.63%, respectively. In addition, the lattice spacings for the three samples were determined to be 0.396, 0.405, and 0.392 nm; these correspond to the (1 1 0), (0 2 0), and (-1 1 1) planes, respectively, of $LiVP_2O_7$.

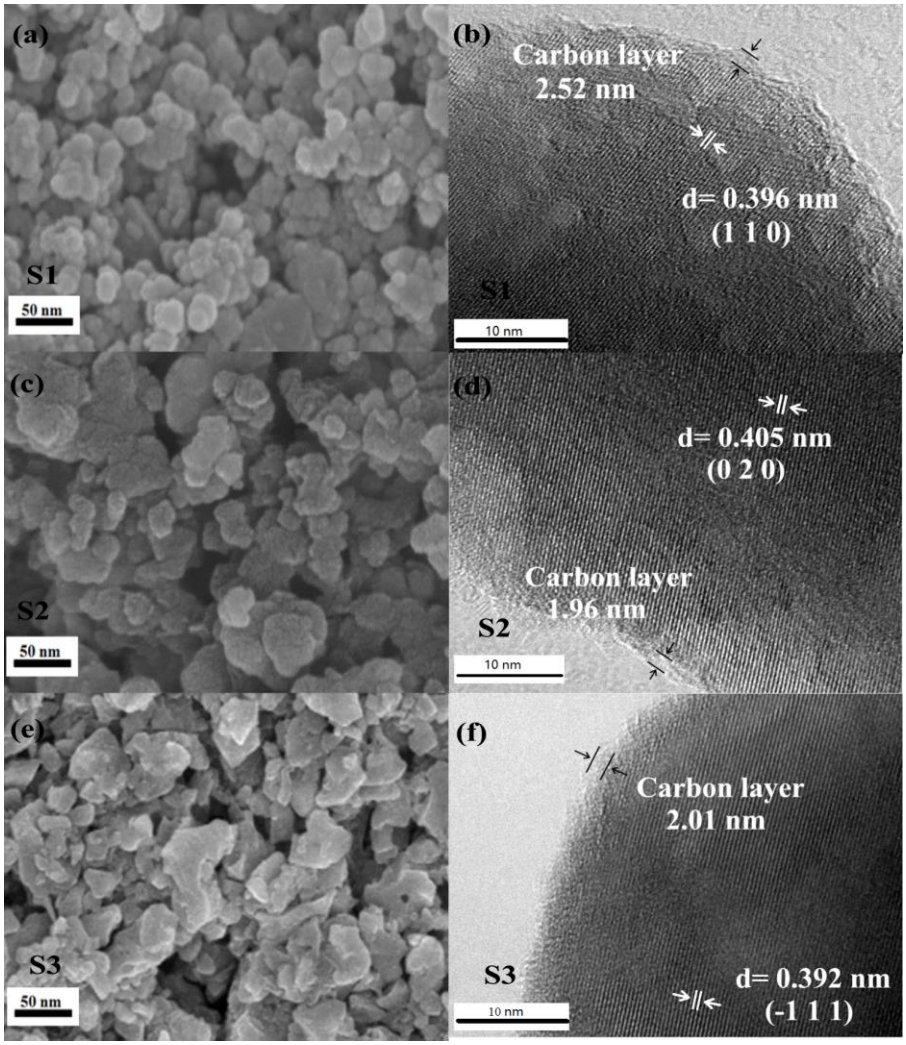

Figure 2. SEM and TEM images of $LiVP_2O_7$/C samples (S1 to S3)

The elemental oxidation states of the $LiVP_2O_7$/C samples were characterized by XPS. The P2p, C1s, V2p, and O1s spectra of the $LiVP_2O_7$/C samples are shown in Fig. 3(a). The oxidation state of V in $LiVP_2O_7$/C was determined based on the XPS V2p spectra shown in Fig. 3(b). Two primary peaks can be observed, at binding energies of 517.08 and 524.48 eV; these can be assigned to $V2p_{3/2}$ and $V2p_{1/2}$. The positions of the peaks are consistent with an oxidation state of +3 [27, 28]. Further, no peaks related to other elements were detected. Based on these results, it can be confirmed that pure $LiVP_2O_7$ was synthesized successfully.

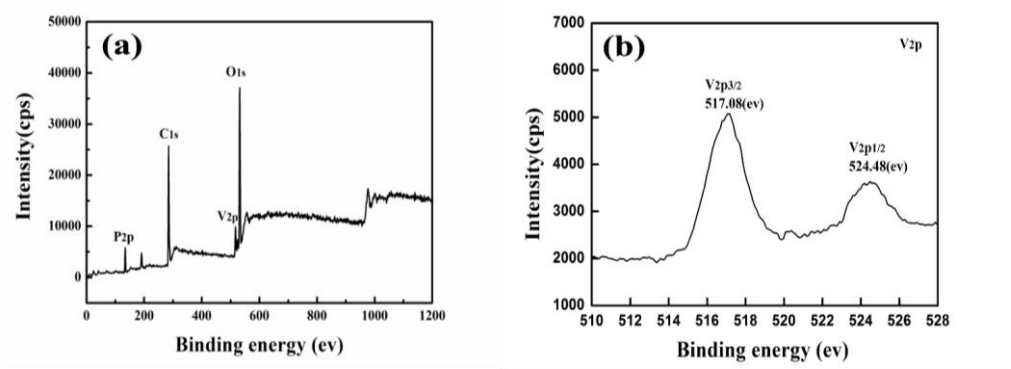

Figure 3. (a) XPS and (b) V2p spectra of $LiVP_2O_7$/C samples

The first charge/discharge curves and cycling performances of S1, S2, and S3 are shown in Fig. 4. A pair of smooth charge/discharge plateaus at approximately 4.3/4.2 V can be seen in Fig. 4(a). The initial discharge capacities of the three samples were 100.2, 102.1, and 87.1 $mAh \cdot g^{-1}$, respectively. After 50 cycles, the discharge capacities decreased to 90.8, 82.1, and 78.1 $mAh \cdot g^{-1}$, respectively, indicating that the performances of the samples declined with cycling. S1 exhibited the highest capacity retention rate. This was consistent with the SEM analyses.

Moreover, Wurm and Zheng both used ball-milling method to synthesize $LiVP_2O_7$ materials and test these samples electrochemical properties, then, found the reversible capacity of these materials were about 50 $mAh \cdot g^{-1}$ (0.05 C) and 46.3 $mAh \cdot g^{-1}$ (0.1 C), respectively [22, 23]. Barker et al used CTR method to prepare $LiVP_2O_7$/C, and reported its first capacity is about 73 $mAh \cdot g^{-1}$ [29]. Kalidas used oxalic dihydrazide (ODH) as carbon source to prepare $LiVP_2O_7$/C, and found the initial discharge capacity is about 95 $mAh \cdot g^{-1}$, the discharge capacity is about 87 $mAh \cdot g^{-1}$ after 50 cycles [30]. So obviously, the electrochemical performance of S1 is better than some papers reported. Details are listed in table 1

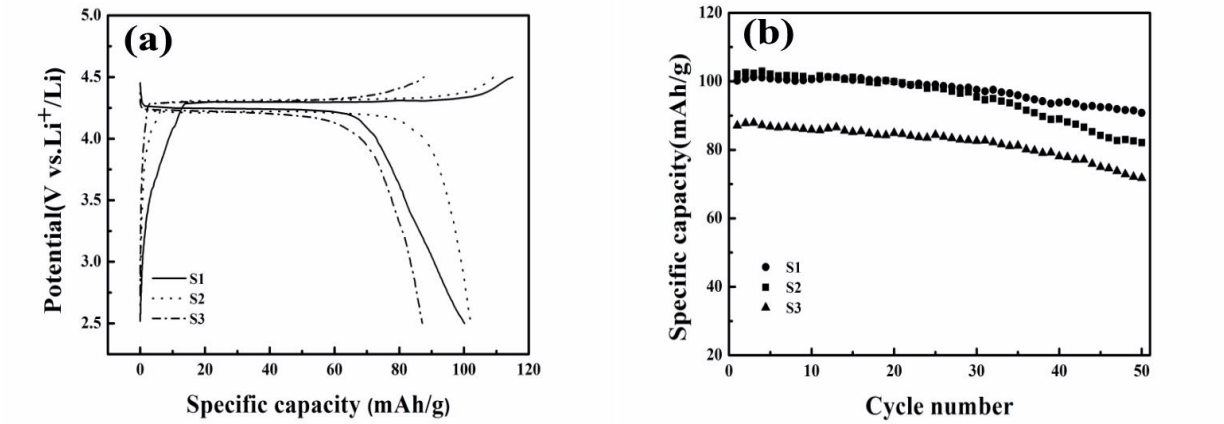

Figure 4. (a) Initial charge/discharge curves and (b) cycling performances of $LiVP_2O_7$/C samples (S1 to S3).

Table 1. Comparison of electrochemical performance of $LiVP_2O_7$ materials (this study and previous reported data).

Authors	Initial discharge capacity ($mAh \cdot g^{-1}$)	50th discharge capacity ($mAh \cdot g^{-1}$)	Rate （C）
Wurm et al. [22]	50	_	0.05
Kalidas et al. [30]	95	87	0.05
Zheng et al. [23]	46.3	_	0.1
Barker et al. [29]	73	_	0.1
S1of this work	100.2	90.8	0.05
S2 of this work	102.1	82.1	0.05
S3 of this work	87.1	78.1	0.05

The CV curves of the three samples are showed in Fig. 5(a)-(c). We can see that the curves exhibit a couple of oxidation/reduction peaks. The oxidation peak at approximately 4.3 V and the reduction peak at approximately 4.2 V correspond to the charge/discharge platforms of the three samples. However, the CV curves for the three test cycles do not overlap completely, indicating that the electrochemical reversibility of the samples needs to be improved. This phenomenon has a determining effect on the cycling performance of the materials.

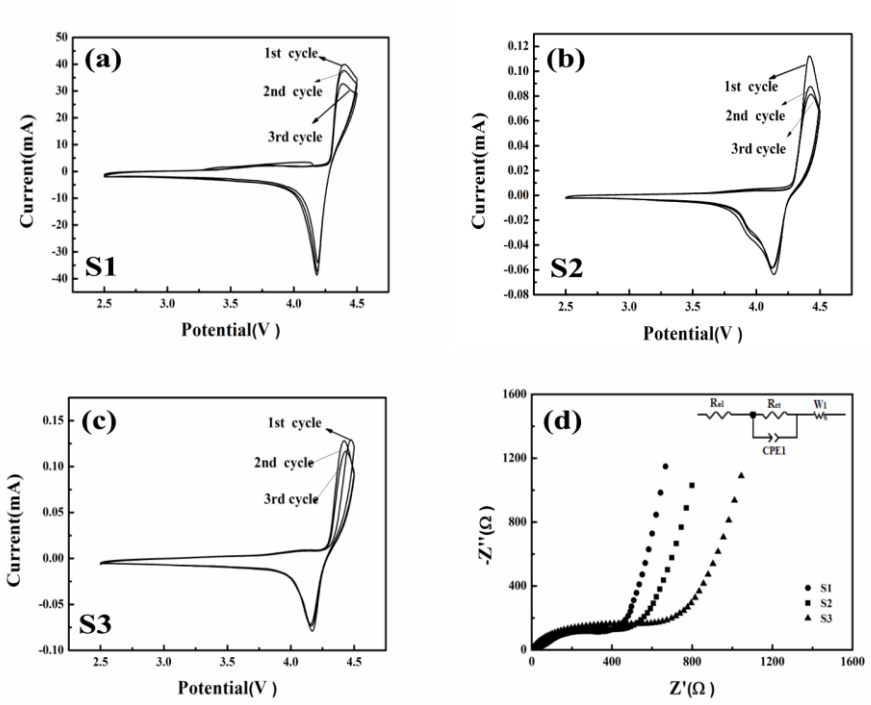

Figure 5. (a) CV and (b) EIS curves of $LiVP_2O_7$/C samples (S1 to S3).

Figure 5(d) displays the typical electrochemical impedance (EIS) spectra of the three samples. Typically, the EIS curve consists of a line intersecting the real axis, a semicircle in the high-frequency region, and a line in the low-frequency region; these components correspond to the resistance of the electrolyte and the electrodes (R_{el}), the charge-transfer resistance (R_{ct}), and the Warburg resistance

(Z_w), respectively. The R_{ct} value is indicative of the ease with which lithium ions can migrate on the cathode surface as well as the impedance of the electrode/electrolyte interface, while Z_w affects the diffusion of the lithium ions in the solid electrode. From the graphs, it is clear that S1 exhibited the lowest electrochemical impedance, while S3 showed the highest impedance, as its larger particles obstructed charge transport.

4. CONCLUSIONS

$LiVP_2O_7$/C was synthesized using a novel two-step synthesis method instead of the conventional high-temperature solid phase method. Moreover, the morphologies and electrochemical properties of $LiVP_2O_7$/C samples prepared using three different precursors were compared. It was found that S1 ($LiVP_2O_7$/C prepared using VP_2O_7 as the precursor) had the smallest particle size and hence the best electrochemical performance, and its first discharge capacity was 100.2 $mAh \cdot g^{-1}$, in addition, its capacity remained at 90.8 $mAh \cdot g^{-1}$ after 50 cycles.

Meanwhile, TEM imaging confirmed that the surfaces of the samples were coated with a carbon layer, which improved the conductivity and enhanced the electrochemical performance of pure $LiVP_2O_7$. In the future, we intend to continue investigating $LiVP_2O_7$ with the aim of further improving its electrochemical performance.

ACKNOWLEDGMENTS
The study was supported by the National Natural Science Foundation of China (No. 21661030)

References

1. G.E. Blomgren, *J. Electrochem. Soc.*, 164 (2017) A5019.
2. J.B. Goodenough, Y. Kim, *Chem. Mater.*, 22 (2014) 587.
3. J.W. Fergus, *J. Power Sources*, 195 (2010) 939.
4. Y.K. Sun, S.T. Myung, B.C. Park, J. Prakash, I. Belharouak, K. Amine, *Nat. Mater.*, 8 (2009) 320.
5. M. Okubo, E. Hosono, J. Kim, M. Enomoto, N. Kojima, T. Kudo, *J. Am. Chem. Soc.*, 129 (2007) 7444
6. I.D. Scott, Y.S. Jung, A.S. Cavanagh, Y. Yan, A.C. Dillon, S.M. George, *Nano Lett.*, 11(2015) 414
7. G. Xu, Z. Liu, C. Zhang, G. Cui, L. Chen, *J. Mater. Chem.*, 3 (2015) 4092.
8. Y.Z. Wang, X. Shao, H.Y. Xu, M. Xie, S.X. Deng, H. Wang, *J. Power Sources*, 226(2013) 140
9. Z. Wang, H. Guo, P. Yan, *Ceram. Int*., 40 (2014)15801.
10. L.X. Yuan, Z.H. Wang, W.X. Zhang, X.L. Hu, J.T. Chao, Y.H. Huang, *Energy Environ. Sci*., 4 (2011) 269.
11. P. Barpanda, S.I. Nishimura, A. Yamada, *Adv. Energy Mater*., 2 (2012) 841.
12. Y. Uebou, S. Okada, M. Egashira, J.I. Yamaki, *Solid State Ionics*, 148 (2002) 323.
13. H. Zhou, S. Upreti, N.A. Chernova, G. Hautier, G. Ceder, M.S. Whittingham, *ChemInform*, 42 (2015) 293
14. S. Lee, S.S. Park, *Chem. Mater*., 24 (2012) 3550.
15. S. Nishimura, M. Nakamura, R. Natsui, A. Yamada, *J. Amer. Chem. Soc*., 132(2010)13596.
16. N. Furuta, S. Nishimura, P. Barpanda, A. Yamada, *Chem. Mater.*, 24(2012)1055.
17. H. Nagano, I. Taniguchi, *J. Power Sources*, 298 (2015) 280.

18. V. Mani, N. Kalaiselvi, *Inorg. Chem*., 55 (2016) 3807.
19. J. Du, L. Jiao, Q. Wu, Y. Liu, Y. Zhao, L. Guo, *Electrochim. Acta,* 103 (2013) 219.
20. J. Xu, S.L. Chou, Q.F. Gu, M.F.M. Din, H.K. Liu, S.X. Dou, *Electrochim. Acta*, 141 (2014) 195.
21. M. Hasumi, I. Taniguchi, *Mater. Lett*., 134(2014) 202.
22. C. Wurm, M. Morcrette, G. Rousse, L. Dupont, C. Masquelier, *Chem. Mater*., 14 (2002) 2701.
23. J.C. Zheng, Y.D. Han, L.B. Tang, B. Zhang, *Electrochim. Acta*, 198 (2016) 195.
24. H. Yu, Z. Su, L. Wang, *Ceram. Int*., 43 (2017) 17116.
25. X.H. Rui, C. Li, C.H. Chen, *Electrochim. Acta*, 54(2009) 3374.
26. J. Yan, W. Yuan, H. Xie, Z.Y. Tang, W.F. Mao, L. Ma, *Mater. Lett*., 71(2012) 1
27. Q. Chen, J. Wang, Z. Tang, W. He, H. Shao, J. Zhang, *Electrochim. Acta*, 52(2007) 5251.
28. J.S. Huang, L. Yang, K.Y. Liu, *Mater. Chem. Phys.*, 128 (2011) 470.
29. J. Barker, R.K.B. Gover, P. Burns, A. Bryan, *Electrochem. Solid-State Lett*., 8 (2005) A446.
30. N. Kalidas, K. Nallathamby, M. Minakshi, *ECS Trans*., 50 (2013) 79.

© 2018 The Authors. Published by ESG (www.electrochemsci.org). This article is an open access article distributed under the terms and conditions of the Creative Commons Attribution license (http://creativecommons.org/licenses/by/4.0/).